ce/papers Proceedings in civil engineering

Ernst & Sohn A Wiley Brand

9TH INTERNATIONAL CONFERENCE ON COMPOSITE CONSTRUCTION IN STEEL AND CONCRETE
M. Knobloch, U. Kuhlmann, W. Kurz, M. Schäfer. (Eds.)
Stromberg, Germany, July 26-30, 2021

# COMPOSITE BRIDGES WITH CRACKED CONCRETE DECK SPANNING BETWEEN TRANSVERSE BEAMS UNDER FATIGUE SHEAR LOADING

**Lena Stempniewski*, Ulrike Kuhlmann***

* Institute of Structural Design, University of Stuttgart
e-mails: lena.stempniewski@ke.uni-stuttgart.de, sekretariat@ke.uni-stuttgart.de

**Keywords**: composite bridges, cracked concrete deck, fatigue, shear loading.

**Abstract.** *For concrete deck of large steel-concrete composite road bridges cracking occurs due to tension because of negative bending moments at the support area, at the same time traffic load with high wheel loads passes the deck spanning between transverse beams. They induce cyclic shear loading in the cracked concrete deck. In composite bridges the application of prefabricated concrete elements has led to economical designs with a benefit in construction time. In this case, the prefabricated concrete elements are supported by the transverse beams when the on-site concrete is poured. For this construction, the concrete is subjected to tension forces resulting from the global load-carrying effect, which needs to be superimposed with local effects as wheel loads acting as shear fatigue loading. In this paper, the fatigue strength of cracked concrete deck under tension and shear fatigue loading is discussed.*

## 1 INTRODUCTION

In coming years numerous large road bridges with spans of 50 - 60 m and more need replacement in Germany. For this span range, steel composite structures proved to be an economical concept for the superstructures. Recently, pre-fabricated concrete elements have increasingly been used for the erection of the concrete deck leading to a more economic and faster manufacturing of the decks. In this case a transversely oriented steel structure is required to support the prefabricated concrete elements. One development in recent years, which is the focus of the research described here, is the arrangement of transverse beams also as cantilever for supporting the prefabricated elements and thus predominantly concrete decks spanning longitudinally. As an example of this construction *Heidingsfeld viaduct* is shown in Figure 1.

Figure 1. Heidingsfeld viaduct (A3) in construction stage

As a result of the global structural behaviour, for the design of composite bridges with transverse beams, the concrete deck is subjected to tension due to the negative bending moment in the support area. Due to the tensile stress in the concrete, cracks often appear over the entire height of the concrete deck even in the



https://doi.org/10.1002/cepa1914




Funding Statement: Open Access funding enabled and organized by Projekt DEAL.
UNIVERSITAET STUTTGART

serviceability state. These cracks are passed by cyclic wheel loads inducing transverse forces in the concrete deck. In this case, the global tensile effects in the deck need to be superimposed with local cyclic shear loading transferred between the cross beams. The results of a current research project funded by the Ministry of Transport and Digital Infrastructure [1] addressing this situation are presented in the paper.

## 2 REINFORCED CONCRETE SLABS UNDER TENSILE STRESSES WITHOUT SHEAR REINFORCEMENT UNDER FATIGUE LOADING

Whilst the static behaviour of cracked reinforced concrete decks without shear reinforcement under direct shear loading has already been investigated by an experimental test programme [2] and the corresponding rules were included in Eurocode 4 (EC4-2, 6.2.2.5 (3)) [3], the fatigue behaviour still needs clarification. The influence of vertical fatigue shear loading on the behaviour of cracked concrete decks has not yet been investigated sufficiently. Separation cracks are induced by tensioning of the concrete. As a result of repeated shear stress the state of the concrete may change, e.g. a failure starting from the tension cracks might be initiated. In addition, the cracks may reduce the dowel effect of the longitudinal reinforcing bars to a greater extent, and the bond zone between concrete and reinforcing steel may also fail.

To determine the load-bearing behaviour of longitudinally reinforced concrete decks under tensile stress without shear reinforcement, a test matrix has been developed to determine S-N diagrams under vertical shear fatigue loading, see chapter 4. First, for each test series a static test is realised in order to determine the maximum load capacity and to compare the behaviour under static and fatigue loading. Then, fatigue tests are conducted in order to determine a S-N-diagram. The outcome of these tests will be further discussed in this paper.

## 3 SHEAR STRENGTH OF REINFORCED CONCRETE MEMBERS WITHOUT TRANSVERSE REINFORCEMENT

### 3.1 Mechanisms of the shear force transfer

The shear force transfer in reinforced concrete members without shear reinforcement has several load-bearing components that influence and superimpose each other. A number of publications and dissertations [2], [4], [5], [6] point out the following load-bearing effects, see Figure 2 and Figure 3:

- Shear force transfer in the non-cracked concrete of the compression zone due to bending $V_{c,c}$
- Dowel action of the longitudinal reinforcement $V_{c,d}$
- Aggregate interlock forces $V_{c,r}$ leading to crack interlocking
- Residual tensile strength of concrete in the fracture process zone
- Direct compression strut in the area of supports

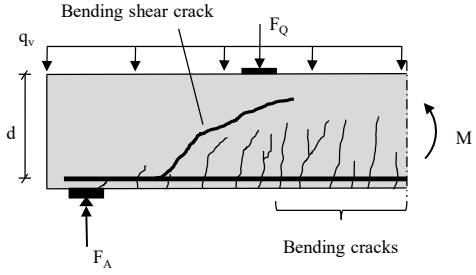


Figure 2. Bending shear crack in a beam without shear reinforcement according to [7]

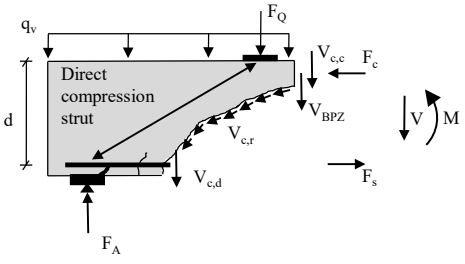


Figure 3. Mechanisms of shear force transfer according to [7]

### 3.2 Normative rules according to EN 1992 and 1994

The verification of the fatigue strength of structural components of reinforced concrete without shear force reinforcement of EN 1992 [8], [9] is based on the CEB Bulletin 188 [10] and the fib Model Code 1990 [11] and 2010 [12]. The rules are based on the assumption that the cracking behaviour under fatigue loading is similar to that under static loading. There is a relationship between static and alternating stress capacity, i.e. the verification under fatigue is carried out by a reduction of the static load-bearing capacity [6].

The static vertical shear force bearing capacity of a structural component without shear force reinforcement is calculated according to EN 1992-2 [8], [9] as given by equation (1). The influence of a normal force is considered in this equation by the stress $\sigma_{cp}$.

$$V_{Rd,c} = \left[C_{Rd,c} \cdot k \cdot \left(100 \cdot \rho_l \cdot f_{ck}\right)^{1/3} + k_1 \cdot \sigma_{cp}\right] \cdot b_w \cdot d \tag{1}$$

With a minimum of:

$$V_{Rd,c} \geq \left(v_{min} + k_1 \cdot \sigma_{cp}\right) \cdot b_w \cdot d \tag{2}$$

where:

| | |
|---|---|
| $f_{ck}$: | Characteristic compressive cylinder strength of concrete at 28 days [N/mm²] |
| k: | $k = 1 + \sqrt{200 / d}$; d in [mm] |
| d: | effective depth of a cross-section [mm] |
| $\rho_l$: | $\rho_l = A_{sl} / (b_w \cdot d) \leq 0{,}02$ [-] |
| $A_{sl}$: | is the area of the tensile reinforcement, which extends ($l_{bd}$ + d) beyond the section considered |
| $b_w$: | is the smallest width of the cross-section in the tensile area [mm] |
| $\sigma_{cp}$: | $\sigma_{cp} = N_{Ed} / A_c < 0{,}2 \cdot f_{cd}$<br>for tensile stress in composite members acc. to EN 1994-2 [3] (tensile stress $\sigma_{cp} < 0$): $\sigma_{cp} = N_{Ed} / A_c > -1{,}85$ N/mm² |
| $N_{Ed}$: | is the axial force in the cross-section due to loading or prestressing [N] ($N_{Ed} > 0$ for compression). The influence of imposed deformations on $N_{Ed}$ may be ignored. |
| $A_c$: | Is the area of concrete cross section [mm²] |

The values of $C_{Rd,c}$, $v_{min}$ and $k_1$ are given in the corresponding National Annex. The recommended value for $C_{Rd,c}$ is $0{,}18/\gamma_c$ that for $v_{min}$ is given by eq. (3) and that for $k_1$ is 0,15.

$$v_{min} = 0{,}035 \cdot k^{3/2} \cdot f_{ck}^{1/2} \tag{3}$$

According to the German National Annex DIN EN 1992-1-1 NA [8] and EN 1994-2 [3]: The recommended value for $C_{Rd,c}$ is $0{,}15/\gamma_c$ that for $v_{min}$ is given by eq. (4) and (5) and that for $k_1$ is 0,12.

$$v_{min} = 0{,}525/\gamma_c \cdot k^{3/2} \cdot f_{ck}^{1/2} \quad \text{for } d \leq 600 \text{ mm} \tag{4}$$

$$v_{min} = 0{,}0375/\gamma_c \cdot k^{3/2} \cdot f_{ck}^{1/2} \quad \text{for } d > 800 \text{ mm} \tag{5}$$

For 600 mm < d ≤ 800 mm interpolation is allowed.

In EN 1992-2 [8], [9] therefore, the minimum and maximum shear forces occurring are related to the static vertical shear force bearing capacity. For structural elements without a shear force reinforcement a sufficient resistance to fatigue may be assumed, if the conditions according to equation (6) or (7) are met. By graphing the equations, a Godman diagram [8] is obtained that clearly displays the permissible ranges, as shown in Figure 4.

$$\text{For } V_{Ed,min}/V_{Ed,max} \geq 0: \frac{|V_{Ed,max}|}{|V_{Rd,c}|} \leq 0{,}5 + 0{,}45 \cdot \frac{|V_{Ed,min}|}{|V_{Rd,c}|} \quad \begin{matrix} \leq 0{,}9 \text{ up to C50/60} \\ \leq 0{,}8 \text{ greater than C55/67} \end{matrix} \tag{6}$$

$$\text{For } V_{Ed,min}/V_{Ed,max} < 0: \frac{|V_{Ed,max}|}{|V_{Rd,c}|} \leq 0{,}5 - \frac{|V_{Ed,min}|}{|V_{Rd,c}|} \tag{7}$$

where:

$V_{Ed,max}$: is the design value of the maximum applied vertical shear force under frequent load Combination

$V_{Ed,min}$: is the design value of the minimum applied shear force under frequent load combination in the cross-section where $V_{Ed,max}$ occurs

$V_{Rd,c}$: is the design value for shear-resistance according to eq. (1)

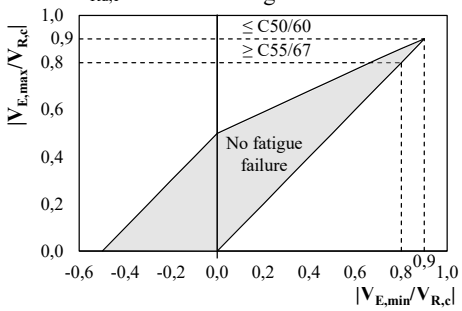


Figure 4. Godman-diagram according to EN1992 [8]

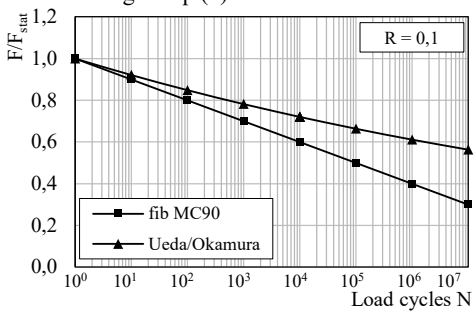


Figure 5. S-N diagram according to the fib model code [11], [12] and Ueda/Okamura [15]

The influence of tensile axial stresses (i.e. with cracked cross-sections) has not yet been considered in the verification under fatigue. Since neither experimental data nor a mechanical model are available, a more stringent verification of the crack width is currently required (see [13] and DIN EN 1994-2/NA, NDP to 7.4.1 (4) [3]).

### 3.3 S-N diagram according fib model code 1990 [11] and 2010 [12] and Ueda/Okamura [15]

The fatigue check of reinforced concrete components without shear force reinforcement is considered to have been carried out if the number of load cycles during the service life n is less than or equal to the maximum tolerable number of cycles to failure N.

$$n \leq N \tag{8}$$

In Model Code 1990 [11] and 2010 [12], a linear relationship is assumed between the ratio of the maximum load to the static shear force bearing capacity and the number of failure cycles N, see Figure 5. The number of cycles to failure are determined as follows:

$$\log N = 10 \cdot (1 - V_{max}/V_{ref}) \tag{9}$$

where:

$V_{max}$: is the maximum shear force under the relevant representative values of permanent loads including prestress and maximum cyclic loading

$V_{ref}$: Vertical shear capacity of a component without shear reinforcement; $V_{ref} = V_{Rd,c}$
Model Code 1990: $V_{ref} = 0{,}12 \cdot \xi \cdot (100 \cdot \rho \cdot f_{ck})^{1/3} \cdot b_{red} \cdot d$
Model Code 2010: $V_{Rd,c} = k_v \cdot \sqrt{f_{ck}}/\gamma_c \cdot z \cdot b_w$

$\xi$: $\xi = 1 + \sqrt{200 / d}$; d in [mm]

$\rho$: Degree of longitudinal reinforcement

$f_{ck}$: Characteristic concrete compressive strength [N/mm²]
(Model Code 1990: $f_{ck} \leq 50$ N/mm²; Model Code 2010: $\sqrt{f_{ck}} \leq 8$ N/mm²)
$b_{red}$: Width of the cross-section minus clamping channels [mm]
d: effective depth of a cross-section [mm]
$k_v$: Components without significant normal force stress with $f_{yk} \leq 600$ N/mm², $f_{ck} \leq 70$ N/mm² and $d_g \geq 10$ mm (Level I):

$$k_v = \frac{180}{1000 + 1{,}25\, z}$$

Level II:

$$k_v = \frac{0{,}4}{1 + 1500\varepsilon_x} \cdot \frac{1300}{1000 + k_{dg} \cdot z}$$

$k_{dg}$: $k_{dg} = \frac{32}{16+d_g} \geq 0{,}75$
$d_g$: Largest grain size of the aggregate [mm]
z: lever arm z = 0,9 d
$\varepsilon_x$: mid-depth strain at the control section;

$$\varepsilon_x = \frac{1}{2 \cdot E_S \cdot A_S} \cdot \left[\frac{M_{Ed}}{z} + V_{Ed} + N_{Ed}\left(\frac{1}{2} \pm \frac{\Delta e}{z}\right)\right] \leq 3{,}0 \cdot 10^{-3}$$

$N_{Ed}$: axial (normal) force (positive for tension)

This approach was extended by Ueda and Okamura [15] on the basis of their own experiments to consider influences from the ratio R of the minimum to maximum load on the total number of cycles, see eq. (10). The relationship is shown graphically in Figure 5.

$$\log(V_{max}/V_{ref}) = -0{,}036 \cdot (1 - R^2) \cdot \log N \qquad (10)$$

where:

R: $R = F_{min}/F_{max}$
$F_{min}$: minimum applied force under cyclic load
$F_{max}$: maximum applied force under cyclic load

## 4 EXPERIMENTAL TEST PROGRAM AND PROCEDURE

### 4.1 Overview of the experimental tests

For a more detailed investigation of the load-bearing behaviour of the cracked concrete slabs under vertical shear force loading, fatigue tests are conducted. 9 tests with identical geometry are tested under fatigue loading with variable stress ratio to define a basic S-N diagram (series S), see Table 1. In addition, a static test is also carried out allowing a direct link to previous research findings (see [2]). Based on the static test the applied load in the fatigue tests may be determined, as the fatigue strength is dependent on the static strength. All fatigue tests are conducted with a frequency of the transverse load of 3,5 Hz and a ratio of minimum to maximum applied load ($R = F_{min}/F_{max}$) of 0,1.

Table 1: Test series S: static and cyclic tests with varied parameters.

| Series number | Axial stress | $R = F_{min}/F_{max}$ | Maximum transverse load $F_{max}$ | Frequency f [Hz] |
|---|---|---|---|---|
| S-01 | $\sigma_N = f_{ctm} A_c$ | - | $F_{ult}$ | Static loading |
| S-02 | $\sigma_N = f_{ctm} A_c$ | 0,1 | 0,6* | 3,5 |
| | | | 0,7 | |
| S-03 | $\sigma_N = f_{ctm} A_c$ | 0,1 | 0,7 | 3,5 |
| S-04 | $\sigma_N = f_{ctm} A_c$ | 0,1 | 0,7 | 3,5 |
| S-05 | $\sigma_N = f_{ctm} A_c$ | 0,1 | 0,65 | 3,5 |
| S-06 | $\sigma_N = f_{ctm} A_c$ | 0,1 | 0,6 | 3,5 |
| S-07 | $\sigma_N = f_{ctm} A_c$ | 0,1 | 0,6 | 3,5 |
| S-08 | $\sigma_N = f_{ctm} A_c$ | 0,1 | 0,65 | 3,5 |
| S-09 | $\sigma_N = f_{ctm} A_c$ | 0,1 | 0,42* | 3,5 |
| | | | 0,5* | |
| | | | 0,7 | |
| S-10 | $\sigma_N = f_{ctm} A_c$ | 0,1 | 0,55* | 3,5 |
| | | | 0,65 | |

* This load level did not cause any signs of failure of the specimen. Thus, the loads were increased in order to initiate failure of the specimen.

### 4.2 Geometry of the test specimens

The aim of the tests is to cause shear failure of the test specimen. However, the shear and bending capacity depend on the same parameters such as concrete compressive strength, longitudinal reinforcement ratio and the geometry of the specimen [16]. Therefore, the load capacity of shear and bending failure are directly related. As a result, it is necessary to determine these parameters very carefully to really achieve shear failure. For this purpose, the geometry especially the shear slenderness a/d must be chosen in harmony with the longitudinal reinforcement ratio. In particular, the shear slenderness a/d should be in a range leading neither to a bending failure (a/d < 6) nor to a shear failure as a result of a direct compression strut into the support (a/d > 2,0 (EN 1992 [8], [9] or 3,0 [17]).

Kani [17] compared the loads in case of shear failure and of bending failure. The quotient of flexural to shear failure can be given as a function of the longitudinal reinforcement ratio and the shear slenderness. The range, in which shear force failure becomes decisive, is referred to by Kani as the "valley of diagonal failure". In this case, the bending tensile reinforcement usually are not fully utilised.

A similar procedure was carried out as a parametric study to determine the failure mode of the test specimens depending on the shear slenderness and the longitudinal reinforcement ratio. Thus, the failure mode may be determined for different levels of shear slenderness and ratios of longitudinal reinforcement. The utilisation may be calculated as a function of those, see Figure 6. In order to achieve the widest possible parameter range, a/d must be chosen as small as possible, but at the same time failure due to a direct compression strut into the support should be avoided. Therefore, a/d has to be chosen as large as possible: a shear slenderness of a/d = 4 has been selected.

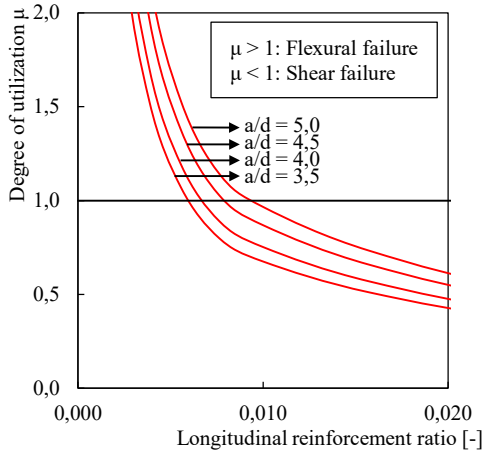


Figure 6. Shear valley for the selected test specimen geometry as a function of the shear slenderness a/d and the longitudinal reinforcement ratio. [1]

Finally, the reinforcement for the standard specimen is selected with 5 Ø 20 mm at 8 cm spacing according to ZTV-ING [18]. With the selected degree of longitudinal reinforcement, a shear failure can be assumed with a shear slenderness of 4. The final geometry of the test specimen (standard specimen, series S) is given in Figure 7.

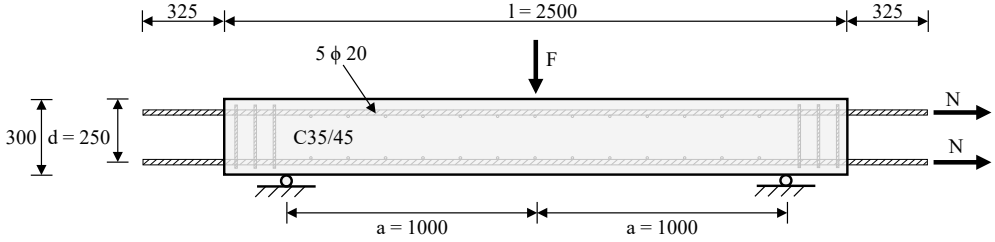


Figure 7. Geometry of the test specimen (standard specimen, test series S).

### 4.3 Test procedure

Prior to the start of the beam tests the compressive and tensile strengths were determined. Based on the tensile concrete strength the axial force was defined as $N = 2\ f_{ctm}\ A_C$. In the first step of the beam tests, the tensile axial force is introduced to the test specimen leading to separation cracks. Therefore, a completed crack pattern is achieved. Afterwards the test specimen is unloaded. In the next step, the normal force is increased to the planned axial force (for test series S: $N = f_{ctm}\ A_C$) and kept constant during the rest of the test. Finally, the transverse load is increased stepwise up to the upper load limit during fatigue tests or until failure in static tests. In fatigue tests, the cyclic transverse loading is started afterwards. The upper load limit in the fatigue tests is determined based on the results of the static reference test.

### 4.4 Experimental test setup

Figure 8 shows the test setup. The axial tensile force as well as the shear load are applied to the test specimen by a frame construction. For the application of the axial tensile force, reinforcement rods with a rolled-up thread are used, that are guided through the test specimen and connected to the frame. The vertical shear load is applied to the centre of the test specimen via a portal frame with hydraulic cylinder, resulting in a symmetrical system with equal shear slenderness on both support sides.

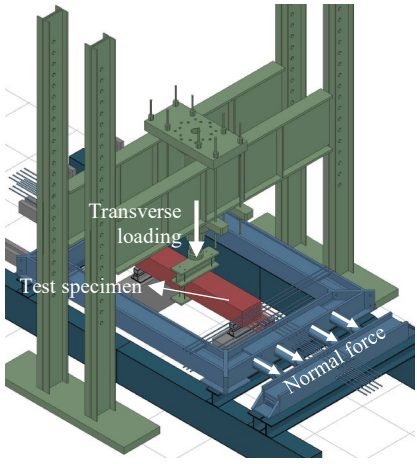


Figure 8. Test set-up

## 5 RESULTS OF THE BEAM TESTS OF SERIES S

### 5.1 Static beam test S-01

In a first step, separation cracks were generated under pure tensile stress and then relieved again. A tensile normal force of $N = 2\ f_{ctm}\ A_C$ was applied in order to induce separation cracks. Separation cracks were generated at regular intervals and with a crack width of 0,2 mm.

In the second step, the normal force was kept constant at $N = f_{ctm}\ A_C$ during the rest of the test. Subsequently the transverse load was applied. Figure 11 shows the deflection in mid span over the machine load (see Figure 9). Up to the maximum, the load was increased continuously (Figure 11, ①) and almost linear, until the maximum load was reached (Figure 11, ②). The shear crack occurred suddenly and without prior notice (see Figure 13). After the shear crack occurred, the load dropped. The load increased then again (Figure 11, ③). The strains with Fibre Bragg Grating-sensors (FBG-sensors) along the lower reinforcement layer increased strongly in the area of the shear crack (see Figure 10 and Figure 12, sensor D10). The loads were still transferred via the dowel action of the longitudinal reinforcement. Subsequently, a transverse crack occurred on the bottom of the specimen (see Figure 14), which led to the failure of the bond between the concrete and reinforcement and finally the failure of the specimen (Figure 11, ④).

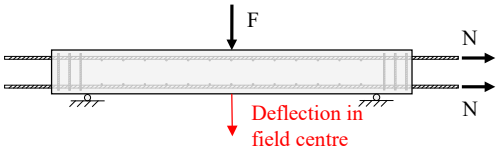


Figure 9. Measurement of the deflection in field centre.

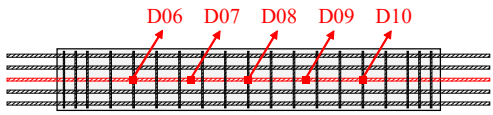


Figure 10. Measurement of the strain in the lower reinforcement.

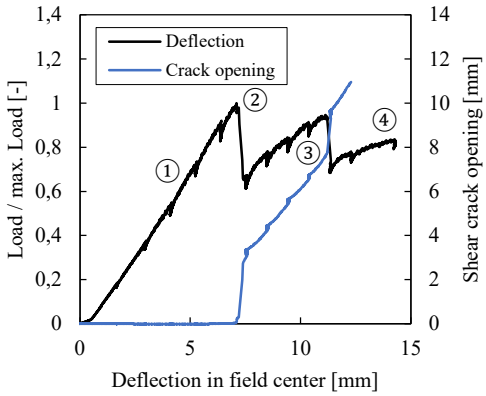


Figure 11. Load-deflection diagram (test S-01).

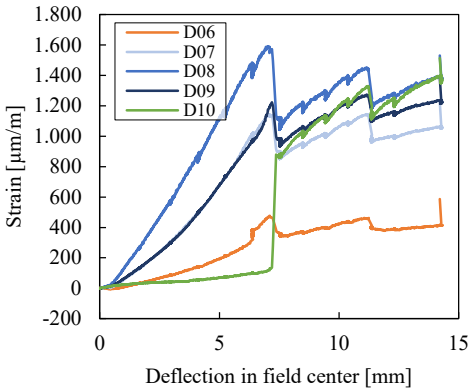


Figure 12. Strain due to transverse loading in the lower reinforcement vs. deflection in field centre (test S-01).

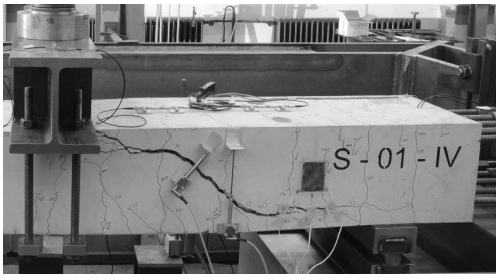


Figure 13. Failure of test specimen S-01 (static test).

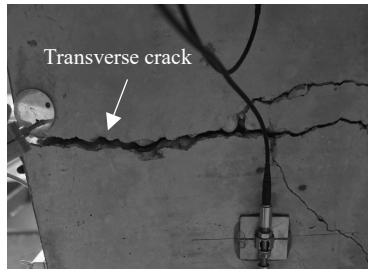


Figure 14. View from below (test S-01).

### 5.2 Fatigue beam tests S-02 to S-10

In the fatigue tests, also separation cracks were generated in the first step by purely axial loading. A tensile axial force of $N = 2\ f_{ctm}\ A_C$ was applied. Separation cracks were generated at regular intervals and with an average crack width of 0,2 mm. In the next step, the axial force was kept constant at $N = f_{ctm}\ A_C$ for the rest of the test. Subsequently the transverse load was applied in a cyclic constant amplitude mode. In the following, the course of test S-08 is presented exemplarily. Figure 15 shows the deflection in the centre span over number of load cycles. Before the first shear crack occurred at approximately 83.200 load cycles on side III, the deflection remained constant. When the shear crack occurred (Figure 15, ①), the deflection increased. The strain in the area of the shear crack increased strongly (sensor D06 in Figure 16). In the further course of the test, the deflection remained almost constant (Figure 15, ②), but the shear crack opening increased (see Figure 15). At approximately 666.455 load cycles, a second shear crack appeared on side IV, cf. Figure 17, leading strongly increasing deflections (Figure 15, ③) as well as the strains in sensor D10 (see Figure 16). Finally, also a transverse crack occurred at the bottom of the specimens leading to the failure of the bond between the reinforcement and concrete and thus the failure of the specimen (see Figure 18).

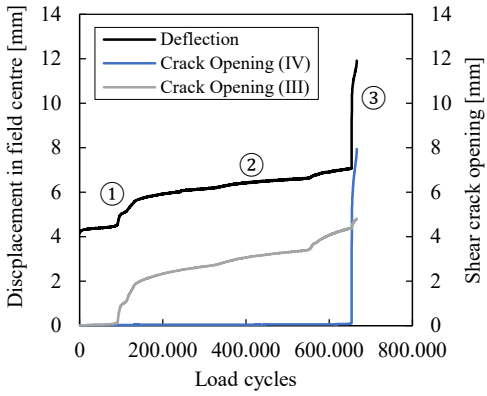


Figure 15. Deflection in field centre vs. load cycles (test S-08).

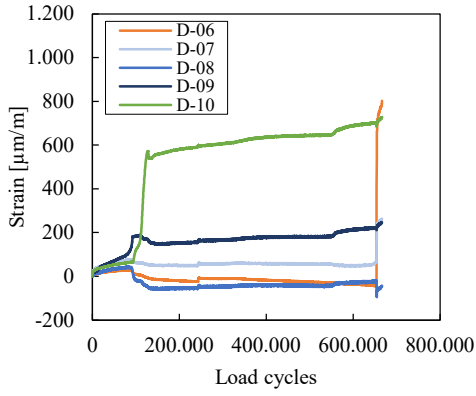


Figure 16. Strain in the lower reinforcement due to transverse loading vs. load cycles (test S-08).

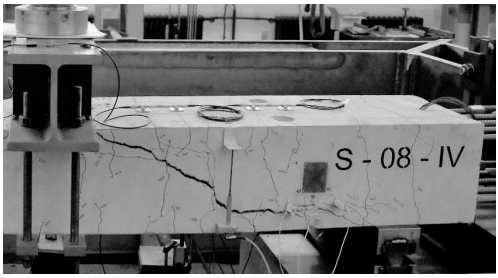


Figure 17. Failure of test specimen S-08 (fatigue test).

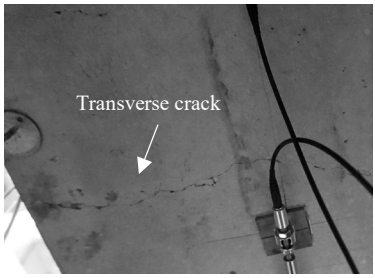


Figure 18. View from below (test S-08).

## 6 ANALYSIS AND EVALUATION OF THE TEST RESULTS

### 6.1 Failure mode and influence of separation cracks

In the static test, the shear crack developed independently of the separation cracks. The failure mode corresponds to the results from the static tests of Ehmann [2]. Here the separation cracks are crossing the shear crack and are not influencing the path of the shear crack. For the corresponding conducted static test S-01 (see Figure 13), the same behaviour was observed. In the fatigue tests, the shear crack has also developed independently of the separation cracks (see e.g. Figure 17). A comparison shows, that the failure mode of the static and fatigue tests is similar. As a result, it may be assumed that the behaviour under fatigue loading is directly linked to static load capacity. Therefore, static and fatigue tests are evaluated together in the S-N-diagram.

### 6.2 S-N diagram

Figure 19 compares the test results in the S-N-diagram according to the fib model code 1990 [11] and 2010 [12] and Ueda/Okamura [15]. The number of load cycles before the first shear crack is plotted on the vertical axis. It can be confirmed that [10], [11] represent a lower bound and [12] an upper bound for the number of load cycles: The test results lie between the two approaches. The test results also show a high scattering, which may also be due to the scattering in the static strength of each test specimen as the fatigue strength highly depends on the static strength.

In Figure 19 some tests are referred to as "run-outs". This refers to the tests S-02, S-09 and S-10. The loading procedure of test S-09 is shown exemplary in Figure 20 as a force-time diagram. This test was started with an upper load of 42% of the static load capacity (0,42 $F_{max}/F_{stat}$). When after 3 million load cycles no signs of failure were visible (Figure 20 ①), the load was increased to 0,5 $F_{max}/F_{stat}$. Even at this level, no failure occurred either, see Figure 20 ②. Therefore, after 1,9 million load cycles, the load was again increased to 0,7 $F_{max}/F_{stat}$, at which failure occurred (Figure 20 ③). The S-N-diagram in Figure 19 shows the three load levels as individual tests, so that test S-09 is found at 0,42, 0,5 and 0,7 $F/F_{stat}$. In test S-10 and S-02 a similar scenario took place: with a maximum load of 0,55 (S-10) resp. 0,6 $F_{max}/F_{stat}$ (S-02), there were no signs of failure at 3 million (S-10) resp. 2,1 million load cycles (S-02), so the load was increased to 0,65 (S-10) resp. 0,7 $F_{max}/F_{stat}$ (S-02). Thus, test specimen S-10 resp. S-02 is both marked as a run-out at 0,55 resp. 0,6 $F/F_{stat}$ and shown at 0,65 resp. 0,7 $F/F_{stat}$ in Figure 19.

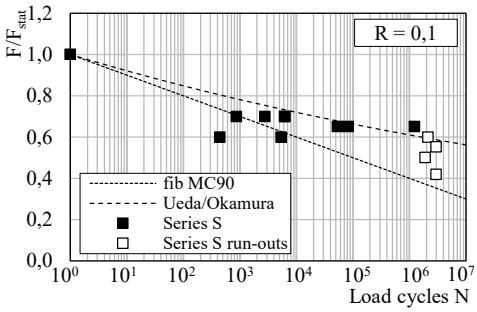


Figure 19. S-N diagram according to the fib model code [11], [12] and Ueda/Okamura [15] with test results of series S from [1]

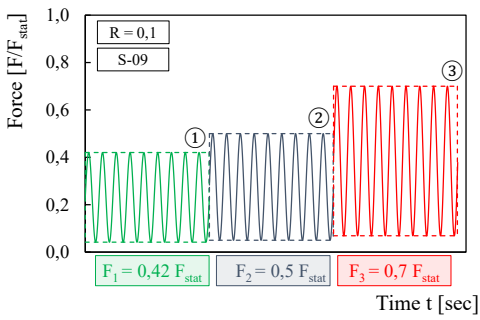


Figure 20. Force-time diagram for test specimen S-09

## 7 SUMMARY AND OUTLOOK

In this paper, tests of reinforced concrete slabs under tensile stresses without shear reinforcement under shear loading were discussed. Fatigue tests as well as a static tests as reference tests were conducted. With the results of the static test, the fatigue loading has been specified, as it is directly connected to the static strength. The test results showed that the failure mechanisms under static and fatigue loading are similar: the separation cracks did not open during fatigue loading. The shear crack was crossing the separation cracks and had developed independently. Further, the test results were evaluated in S-N-diagrams according to the fib model code [11], [12] and Ueda/Okamura [15]. The comparison showed that the results lie in between both approaches. As a conclusion, the fib model code [11], [12] represents a lower limit function for the fatigue strength and Ueda/Okamura an upper one.

Further tests with varying axial forces and longitudinal reinforcement ratios are underway. Furthermore, an additional test series with prefabricated concrete elements is going to be conducted soon. Also, additional tests are planned in order to analyse the effect of realistic varying loading conditions in bridges to check the applicability of the Palmgren-Miner-rule.

## ACKNOWLEDGEMENT

The work presented is carried out as part of the research project [1] of the Federal Ministry of Transport and Digital Infrastructure. The authors wish to thank for that funding. The project [1] is a joint project with colleagues from the Technical University of Berlin, Ingenieurbüro Prof. Dr.-Ing. Ulrike Kuhlmann, GMG Ingenieurgesellschaft and the Technical University of Munich. The authors would like to thank all project partners for the good and fruitful cooperation. Moreover, we thank the Material Testing Institute of the University of Stuttgart for their great support in conducting the tests.

## REFERENCES


[1] Geißler, K.; Kuhlmann, U.; et al., *Wissenschaftlich-technische Untersuchungen zur Feststellung der Ermüdungsfestigkeit der Fahrbahnplatte und der Konsolträger bei Großbrücken in Stahlverbundbauweise mit Halbfertigteilen (Investigations to determine the fatigue strength of the concrete deck and of the cantilever beam for large composite bridges including partially prefabricated deck)*, Report on the research project on behalf of the Federal Ministry of Transport and Digital Infrastructure, Germany (StB17/7192.40/80-3043765), ongoing research project (2019-2021).

[2] Ehmann, J., *Querkraftragfähigkeit zugbeanspruchter Stahlbetonplatten in Verbundbrücken, (Resistance under transverse force of tensioned concrete decks),* Dissertation, Institute of Structural Design, University of Stuttgart, No. 2003-3, 2003.

[3] EN 1994-2, *Eurocode 4: Design of composite steel and concrete structures. Part 2: General rules and rules for bridges*, Brussels, Belgium: Comité Européen de Normalisation, 2005.

[4] ACI-ASCE Committee 445, *Recent Approaches to Shear Design of Structural Concrete: State-of-the-Art-Report by ASCE-ACI Commitee 445 on Shear and Torsion*, ASCE-Journal of Structural Engineering 124, p. 1375-1417.

[5] Hegger, J.; Görtz, S., *Querkrafttragfähigkeit von Stahlbeton- und Spannbetonbalken aus Normal- und Hochleistungsbeton*, Deutscher Ausschuss für Stahlbeton im DIN Deutsches Institut für Normung e.V., Beuth Verlag, Berlin, 2007.

[6] Kohl, M., *Tragverhalten von Stahlbetontragwerken ohne Querkraftbewehrung unter Ermüdungsbeanspruchungen,* Dissertation, Hamburg University of Technology, 2014.

[7] Latte, S., *Zur Tragfähigkeit von Stahlbeton-Fahrbahnplatten ohne Querkraftbewehrung*, Dissertation, Hamburg University of Technology, 2010.

[8] EN 1992-1-1: *Eurocode 2: Design of concrete structures - Part 1-1 : General rules and rules for buildings*, 2011, and German National Annex: DIN EN 1992-1-1/NA: Nationaler Anhang zu Eurocode 2: Bemessung und Konstruktion von Stahlbeton- und Spannbetontragwerken – Teil 1-1: Allgemeine Bemessungsregeln und Regeln für den Hochbau, Beuth Verlag, 2013.

[9] EN 1992-2: *Eurocode 2 - Design of concrete structures - Concrete bridges - Design and detailing rules*, 2010, and German National Annex: DIN EN 1992-2/NA: Nationaler Anhang zu Eurocode 2: Bemessung und Konstruktion von Stahlbeton- und Spannbetontragwerken – Teil 2: Betonbrücken, Beuth Verlag, 2013.

[10] Comité Euro-International du Béton (CEB): Fatigue of Concrete structures, CEB Bulletin d'information, 1988.

[11] Comité Euro-International du Béton (CEB); Fédération Internationale de la Précontrainte (FIP): CEB-FIP Model Code 1990, 1993.

[12] Fédération internationale du béton (fib): fib Model Code for Concrete Structures 2010, 2012.

[13] Federal Ministry of Transport and Digital Infrastructure, *Konstruktions- und Bemessungshinweise für Stahl- und Stahlverbundbrückenkonstruktionen*, Berlin, 2018.

[14] Mager, M.; Geißler, K., *Ersatzneubau der Rader Hochbrücke - Gutachterliche Stellungnahme zur Bauweise mit Konsolträgern und längsgespannter Fahrbahnplatte (1, Teilbericht)*, Report, GMG Ingenieurgesellschaft, Berlin, 2018.

[15] Ueda, T., Okamura, H., *Behavior in shear of reinforced concrete beams under fatigue loading*, Journal of the Faculty of Engineering, Vol. 37, No. 1, The University of Tokyo, 1983.

[16] Zilch, K., Zehetmaier, G., *Bemessung im konstruktiven Betonbau - Nach DIN 1045-1 (Fassung 2008) und EN 1992-1-1 (Eurocode 2)*, 2. Edition, Springer-Verlag, Berlin, 2010.

[17] Kani, G. N. J,. *Basic Facts Concerning Shear Failure*, Journal of the American Concrete Institute, No. 6, p. 675-692, 1966.

[18] *Zusätzliche Technische Vertragsbedingungen und Richtlinien für Ingenieurbauten (ZTV-ING) - Teil 4: Stahlbau, Stahlverbundbau*, Federal Highway Research Institute, 2012.